REPORT DOCUMENTATION PAGE

1. REPORT DATE *(DD-MM-YYYY)*	2. REPORT DATE	3. DATES COVERED *(From - To)*
11-15-2002	Technical	01-06-1997 to 30-11-2000

4. TITLE AND SUBTITLE

Development of a six-degree of freedom simulation model for the REMUS autonomous underwater vehicle

5a. CONTRACT NUMBER

5b. GRANT NUMBER
N00014-97-1-0787

5c. PROGRAM ELEMENT NUMBER

6. AUTHOR(S)

Timothy Prestero

5d. PROJECT NUMBER

5e. TASK NUMBER

5f. WORK UNIT NUMBER

7. PERFORMING ORGANIZATION NAME(S) AND ADDRESS(ES)

Woods Hole Oceanographic Institution
Woods Hole, MA 02543

8. PERFORMING ORGANIZATION REPORT NUMBER

N/A

9. SPONSORING/MONITORING AGENCY NAME(S) AND ADDRESS(ES)

Office of Naval Research
EnvironmentalSciences DIrectorate
Arlington, VA 22217-5660

10. SPONSOR/MONITOR'S ACRONYM(S)

11. SPONSORING/MONITORING AGENCY REPORT NUMBER

12. DISTRIBUTION AVAILABILITY STATEMENT

APPROVED FOR PUBLIC RELEASE – DISTRIBUTION IS UNLIMITED

20030103 002

14. ABSTRACT

Abstract— This paper describes the development and verification of a six degree of freedom, non-linear simulation model for the REMUS AUV, the first such model for this platform. In this model, the external forces and moments resulting from hydrostatics, hydrodynamic lift and drag, added mass, and the control inputs of the vehicle propeller and fins are all defined in terms of vehicle coefficients. This paper briefly describes the derivation of these coefficients. The equations determining the coefficients, as well as those describing the vehicle rigid-body dynamics, are left in non-linear form to better simulate the inherently non-linear behavior of the vehicle. Simulation of the vehicle motion is achieved through numeric integration of the equations of motion. The simulator output is then verified against vehicle dynamics data collected in experiments performed at sea. The simulator is shown to accurately model the motion of the vehicle. The paper concludes with recommendations for future model validation experiments.

15. SUBJECT TERMS

REMUS AUV, simulation and control, model testing

16. SECURITY CLASSIFICATION OF:			17. LIMITATION OF ABSTRACT	18. NUMBER OF PAGES	19a. NAME OF RESPONSIBLE PERSON
a. REPORT	b. ABSTRACT	c. THIS PAGE			Timothy Prestero
UL	UL	UL	UL	6	19b. TELEPONE NUMBER *(Include area code)* 508.289.6520

Development of a Six-Degree of Freedom Simulation Model for the REMUS Autonomous Underwater Vehicle

Timothy Prestero

MIT/WHOI Joint Program in Oceanographic Engineering

tprester@mit.edu

Abstract— This paper describes the development and verification of a six degree of freedom, non-linear simulation model for the REMUS AUV, the first such model for this platform. In this model, the external forces and moments resulting from hydrostatics, hydrodynamic lift and drag, added mass, and the control inputs of the vehicle propeller and fins are all defined in terms of vehicle coefficients. This paper briefly describes the derivation of these coefficients. The equations determining the coefficients, as well as those describing the vehicle rigid-body dynamics, are left in non-linear form to better simulate the inherently non-linear behavior of the vehicle. Simulation of the vehicle motion is achieved through numeric integration of the equations of motion. The simulator output is then verified against vehicle dynamics data collected in experiments performed at sea. The simulator is shown to accurately model the motion of the vehicle. The paper concludes with recommendations for future model validation experiments.

Keywords—REMUS AUV, Simulation and Control, Model Testing

I. INTRODUCTION

IMPROVING the performance of modular, low-cost autonomous underwater vehicles (AUVs) in such applications as long-range oceanographic survey, autonomous docking, and shallow-water mine countermeasures requires improving the vehicles' maneuvering precision and battery life. These goals can be achieved through the improvement of the vehicle control system. A vehicle dynamics model based on a combination of theory and empirical data would provide an efficient platform for vehicle control system development, and an alternative to the typical trial-and-error method of vehicle control system field tuning. Furthermore, a good vehicle dynamics model is a crucial element of the Kalman filter at the heart of any navigation algorithm. As there exists no standard procedure for vehicle modeling in industry, the simulation of each vehicle system represents a new challenge.

II. THE REMUS AUV

Developed by von Alt and associates at the Woods Hole Oceanographic Institute's Oceanographic Systems Laboratory (WHOI OSL), RE-

MUS (Remote Environmental Monitoring Unit) is a low-cost, man-portable AUV design with approximately 1000 hours of water time over hundreds of missions on 15 vehicles, with applications in autonomous docking, long-range oceanographic survey, and shallow-water mine reconnaissance [14], [15], [16].

The hull shape of the REMUS vehicle is based on the Myring hull profile equations [11], which describe a body contour with minimal drag coefficient for a given fineness ratio (body length/maximum diameter). For reference, Myring [11, p. 189] assumes a total body length of 100 units, and classifies body types by a code of the form $a/b/n/\theta/\frac{1}{2}d$, where θ is given in radians. REMUS is based on the Myring B hull contour, which is given by the code 15/55/1.25/0.4363/5. See Figure 1 for a plot of the REMUS profile, and Figure 2 for a picture of the vehicle.
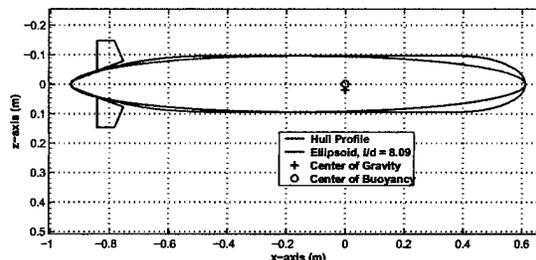

Fig. 1: REMUS Profile (XZ-plane)

Fig. 2: The REMUS AUV

III. VEHICLE MODEL DEVELOPMENT

The standard submarine equations of motion—developed by Gertler and Hagen [7] and revised by

Humphreys [10] and Feldman [4]—offer a general framework for the development of the vehicle equations of motion. In these equations of motion, external forces and moments

$$\sum F_{ext} = F_{hydrostatic} + F_{lift} + F_{drag} + F_{control}$$

are described in terms of vehicle coefficients. For example, vehicle axial drag:

$$F_d = -\left(\frac{1}{2}\rho c_d A_f\right) u \left|u\right| = X_{u|u|} u \left|u\right|$$

where the coefficient

$$X_{u|u|} = \frac{\partial F_d}{\partial(u\,|u|)} = -\frac{1}{2}\rho c_d A_f$$

The vehicle coefficients were derived as follows:
- *Axial Drag* Author tow tank experiments [1].
- *Added Mass* Hydrodynamic theory from Newman [12] and empirical formulae from Blevins [2].
- *Vehicle Crossflow Drag* Hydrodynamic theory from Newman [12] and empirically-derived formulae from Hoerner [8].
- *Vehicle Body Lift* Empirically-derived formulae from Bottaccini [3], Fidler [5] and Hoerner [9].
- *Fin Forces* Empirically-derived formulae from Hoerner [8], [9] and Whicker and Fehlner [17].

The author uses a very simple model for the REMUS propulsion system, which treats the propeller as a source of constant thrust and torque. The values for these coefficients are based on a vehicle forward speed of three knots (1.54 m/s), and were derived from vehicle design-stage propeller bench tests conducted by Ben Allen at WHOI OSL, and from experiments conducted by the author at sea. This simple model is acceptable for small amplitude perturbations about the vehicle steady state. In the future, the author would like to replace this with a more sophisticated propeller model, such as developed by Yoerger and Slotine [18], or with experimentally-derived values.

IV. Modeling Assumptions

The following assumptions were made in the development of the vehicle model:
- *The vehicle is a rigid body of constant mass.* In other words, the vehicle mass and mass distribution do not change during operation.
- *Control surface assumptions.* We assume that the control fins do not stall regardless of angle of attack. We also assume an instantaneous fin response, meaning that that vehicle actuator time response is small in comparison with the vehicle attitude time response.

- *The vehicle is deeply submerged in a homogeneous, unbounded fluid.* In other words, the vehicle is located far from free surface (no surface effects, i.e. no sea wave or vehicle wave-making loads), walls and bottom.
- *The vehicle does not experience memory effects.* The simulator neglects the effects of the vehicle passing through its own wake.

V. Equations of Motion

The vehicle equations consist of the following elements:
- *Kinematics*: the geometric aspects of motion
- *Rigid-body Dynamics*: the vehicle inertia matrix
- *Mechanics*: forces and moments causing motion

For a treatment of the generic vehicle kinematic equations, see Fossen [6].

Combining the equations for the vehicle rigid-body dynamics with the equations for the forces and moments on the vehicle, we arrive at the combined nonlinear equations of motion for the REMUS vehicle in six degrees of freedom. These equations follow the SNAME convention for the assignment of the body-fixed vehicle coordinate system.

Surge, or translation along the vehicle x-axis:

$$
\begin{aligned}
(m - X_{\dot{u}})\dot{u} &+ mz_g\dot{q} - my_g\dot{r} = X_{HS} + X_{u|u|}u\,|u| \\
&+ (X_{wq} - m)wq + (X_{qq} + mx_g)q^2 \\
&+ (X_{vr} + m)vr + (X_{rr} + mx_g)r^2 \\
&- my_g pq - mz_g pr + X_{prop}
\end{aligned}
\tag{1}
$$

Sway, or translation along the vehicle y-axis:

$$
\begin{aligned}
(m - Y_{\dot{v}})\dot{v} &- mz_g\dot{p} + (mx_g - Y_{\dot{r}})\dot{r} = Y_{HS} \\
&+ Y_{v|v|}v\,|v| + Y_{r|r|}r\,|r| + my_g r^2 \\
&+ (Y_{ur} - m)ur + (Y_{wp} + m)wp \\
&+ (Y_{pq} - mx_g)pq + Y_{uv}uv + my_g p^2 \\
&+ mz_g qr + Y_{uu\delta_r}u^2\delta_r
\end{aligned}
\tag{2}
$$

Heave, or translation along the vehicle z-axis:

$$
\begin{aligned}
(m - Z_{\dot{w}})\dot{w} &+ my_g\dot{p} - (mx_g + Z_{\dot{q}})\dot{q} = Z_{HS} \\
&+ Z_{w|w|}w\,|w| + Z_{q|q|}q\,|q| \\
&+ (Z_{uq} + m)uq + (Z_{vp} - m)vp \\
&+ (Z_{rp} - mx_g)rp + Z_{uw}uw + mz_g(p^2 + q^2) \\
&- my_g rq + Z_{uu\delta_s}u^2\delta_s
\end{aligned}
\tag{3}
$$

Roll, or rotation about the vehicle x-axis:

$$
\begin{aligned}
- mz_g\dot{v} &+ my_g\dot{w} + (I_{xx} - K_{\dot{p}})\dot{p} = K_{HS} \\
&+ K_{p|p|}p\,|p| - (I_{zz} - I_{yy})qr \\
&+ m(uq - vp) - mz_g(wp - ur) + K_{prop}
\end{aligned}
\tag{4}
$$

Pitch, or rotation about the vehicle y-axis:

$$
\begin{aligned}
mz_g \dot{u} &- (mx_g + M_{\dot{w}})\dot{w} + (I_{yy} - M_{\dot{q}})\dot{q} = M_{HS} \\
&+ M_{w|w|}w\,|w| + M_{q|q|}q\,|q| \\
&+ (M_{uq} - mx_g)uq + (M_{vp} + mx_g)vp \\
&+ [M_{rp} - (I_{xx} - I_{zz})]\,rp + mz_g(vr - wq) \\
&+ M_{uw}uw + M_{uu\delta_s}u^2\delta_s
\end{aligned}
\tag{5}
$$

Yaw, or rotation about the vehicle z-axis:

$$
\begin{aligned}
-my_g \dot{u} &+ (mx_g - N_{\dot{v}})\dot{v} + (I_{zz} - N_{\dot{r}})\dot{r} = N_{HS} \\
&+ N_{v|v|}v\,|v| + N_{r|r|}r\,|r| \\
&+ (N_{ur} - mx_g)ur + (Nwp + mx_g)wp \\
&+ [N_{pq} - (I_{yy} - I_{xx})]\,pq - my_g(vr - wq) \\
&+ N_{uv}uv + N_{uu\delta_r}u^2\delta_r
\end{aligned}
\tag{6}
$$

Note that the vehicle cross-products of inertia, I_{xy}, I_{xz} and I_{yz}, are assumed to be small and are neglected in the above equations of motion. Similarly, the equations do not include zero-valued coefficients.

VI. NUMERICAL INTEGRATION

The nonlinear differential equations defining the vehicle accelerations and the kinematic equations give us the vehicle accelerations in the different reference frames. Given the complex and highly nonlinear nature of these equations, we will use numerical integration to solve for the vehicle speed, position, and attitude in time.

Consider that at each time step, we can express the vehicle equations of motion as follows:

$$
\dot{x}_n = f(x_n, u_n)
\tag{7}
$$

where x_n is the vehicle state vector:

$$
x_n = [u \ \ v \ \ w \ \ p \ \ q \ \ r \ \ x \ \ y \ \ z \ \ \phi \ \ \theta \ \ \psi]^T
\tag{8}
$$

and u_n is the input vector:

$$
u_n = \begin{bmatrix} \delta_s & \delta_r & X_{\text{prop}} & K_{\text{prop}} \end{bmatrix}^T
\tag{9}
$$

We will use the Runge-Kutta method of numerical integration, for which we first calculate the following:

$$
\begin{aligned}
k_1 &= x_n + f(x_n, u_n) \\
k_2 &= f\left(x + \frac{\Delta t}{2}k_1, u_{n+\frac{1}{2}}\right) \\
k_3 &= f\left(x + \frac{\Delta t}{2}k_2, u_{n+\frac{1}{2}}\right) \\
k_4 &= f(x + \Delta t k_3, u_{n+1})
\end{aligned}
\tag{10}
$$

where the interpolated input vector

$$
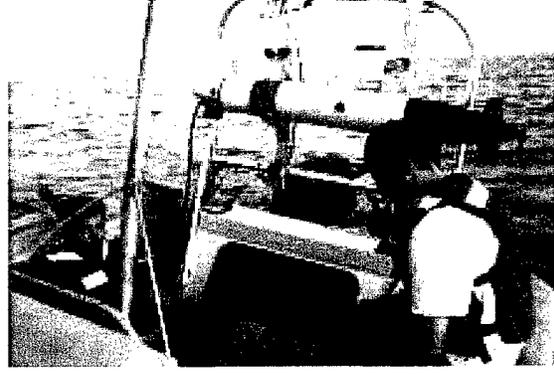u_{n+\frac{1}{2}} = \frac{1}{2}(u_n + u_{n+1})
\tag{11}
$$

Fig. 3: The author (left) and Mike Purcell from WHOI OSL, running vehicle experiments at the Rutgers Marine Field Station in Tuckerton, NJ [*Photo courtesy of Nuno Cruz, Porto University*]

We combine the above equations:

$$
x_{n+1} = x_n + \frac{\Delta t}{6}(k_1 + 2k_2 + 2k_3 + k_4)
\tag{12}
$$

to yield the new vehicle state at each time step.

VII. FIELD EXPERIMENTS

In order to verify the accuracy of the vehicle model, the author conducted a series of experiments at sea measuring the response of the vehicle to step changes in rudder and stern plane angle. These experiments were conducted at both the Woods Hole Oceanographic Institution and at the Rutgers University Marine Field Station in Tuckerton, New Jersey with the assistance of the WHOI OSL staff.

In each experiment at sea we measured the vehicle depth and attitude, represented in the vehicle model by the following, globally-referenced vehicle states:

$$
x = \begin{bmatrix} z & \phi & \theta & \psi \end{bmatrix}^T
\tag{13}
$$

In these experiments we also recorded the vehicle fin angles, represented in the vehicle model by the following vehicle-referenced control inputs:

$$
u_n = \begin{bmatrix} \delta_s & \delta_r \end{bmatrix}^T
\tag{14}
$$

Note that for all of the field tests described in this section, the vehicle propeller was not used as a control input, but was instead kept at a constant 1500 RPM. As propeller thrust and torque were difficult to estimate for different propeller RPMs, sticking to a constant value allowed us to remove a source of uncertainty from the vehicle model comparison.

In order to measure the vehicle response to step changes in fin angle, the vehicle was given the following commands:

452

- *Timer to desired depth* For "pitch up", the vehicle was commanded to six meters depth, to avoid breaking the surface. For "pitch down" commands, the vehicle was commanded to 2 meters depth.
- *Step change in fin angle* Upon achieving depth, the vehicle was commanded to hold a certain fin angle for two seconds in the case of vertical plane response, or longer for horizontal plane response.

The fin angle duration of two seconds was chosen as a result of the experimental run shown in Figure 4. In the depth plot, right around the seven-second mark, you can see that the vehicle ran into and bounced off the bottom. Given the unpredictable vehicle open-loop response, the author thought it wise to use short periods.
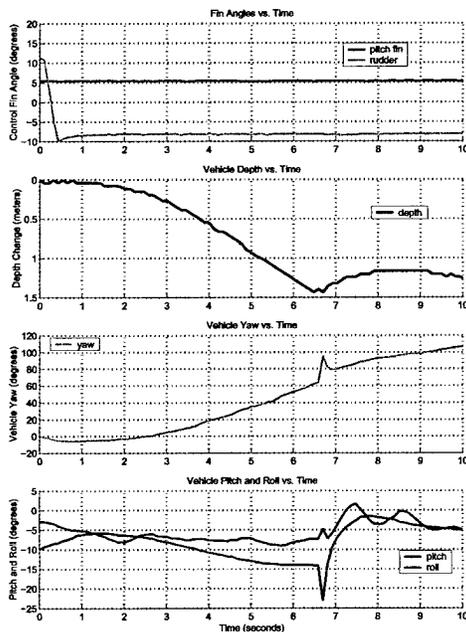

Fig. 4: REMUS Mission Data: Vehicle bounces off the bottom [d980729a, Obj. 6]

From these vehicle experiments, we get measurements for the vehicle response to step changes in rudder and stern plane angle. It is important to note that during straight and level flight, the vehicle operates at a roll offset of negative five degrees ($\phi = -5$) due to the propeller torque. As a result, we never get pure vertical- or horizontal-plane motion. That said, the vehicle roll is small enough that we are still able identify the vehicle behavior in pitch and yaw.

See Figure 5 for REMUS motion while operating under closed-loop control, for comparison with the open-loop, step response data. In the example shown, the vehicle was commanded to maintain a depth of two meters.
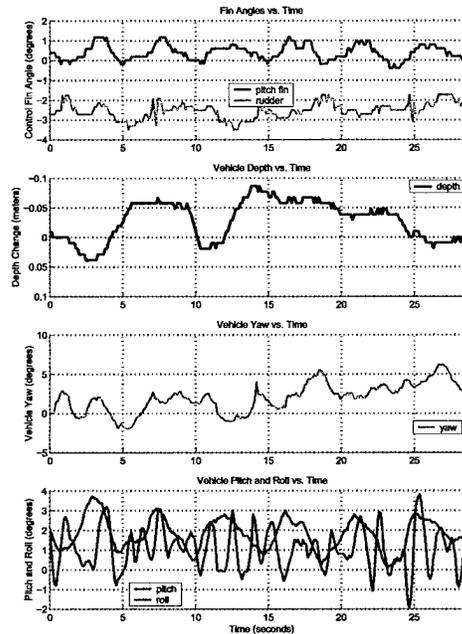

Fig. 5: REMUS Mission Data: Vehicle under closed-loop control. [d990727, Obj. 4]

VIII. MODEL COMPARISON

The model was given initial conditions and fin inputs to match the experimental data. The following uncertainties affected the accuracy of the model comparison:

- *Vehicle Initial Conditions* The greatest uncertainty was the vehicle state at the start of each experimental objective. We were unable to measure currents, wave effects, and non-axial vehicle velocities, which would have all affected the vehicle motion during open-loop maneuvers.
- *Control Fin Alignment* Although the alignment of the vehicle fins was checked before each experimental mission, it was difficult to keep the vehicle control fins from getting knocked during vehicle transportation and launch. This could have resulted in fin misalignments as great as five degrees.
- *Attitude Sensor Dynamics* The vehicle attitude sensor was sensitive to coupling due to vehicle accelerations. Although most likely a small effect, the

453

author did not have the opportunity to characterize these sensor dynamics.

Recommended improvements to the experimental method and instrumentation are discussed in the conclusion.

Figures 6 and 7 show the vehicle response to step changes in rudder angle. In Figure 6, the vehicle was given zero fin inputs for ten seconds, then four degrees of positive rudder for 25 seconds, then four degrees of negative rudder for 30 seconds.

Figure 7 shows a direct comparison of the experiment and simulator data for a period of steady yaw rate (i.e. no initial transients). The simulated vehicle yaw rate is shown to be a very close match to the experiment. Discrepancies between the vehicle depth rates, and vehicle pitch and roll angles likely have to do with differences in the simulator initial conditions.

Figures 8 and 9 show the vehicle response to a step change in pitch fin angle. The vehicle was given zero fin inputs for two seconds, then four degrees of negative pitch fin for two seconds. Figure 9 shows a vehicle depth change of roughly 0.5 meters and a pitch change of twenty degrees, which both compare well with the experimental data..

IX. EXPERIMENTAL RECOMMENDATIONS

The vehicle dynamics data collected in the experiments were limited in the number of vehicle states recorded, and the accuracy of those measurements. This made it difficult to judge the validity of the model comparison.

For future experiments, the author has augmented the standard REMUS sensors with an inertial measurement unit: the Crossbow DMU-AHRS (Dynamic Measurement Unit—Attitude and Heading Reference System). This instrument outputs magnetic orientation, accelerations and angular rates on three axes. This will significantly improve our ability to measure the vehicle initial conditions in particular, and the vehicle motion in general.

Second, even with improved vehicle instrumentation it is still important to understand the vehicle steady-state conditions. AUVs like REMUS can be unstable when operating without control. Using the inertial measurement unit, it will be possible to identify the propeller RPM and fixed fin angles which result in straight and level vehicle flight. These settings will then be used at the start of every experimental run.
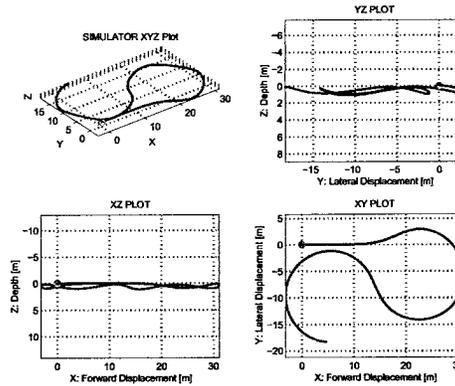

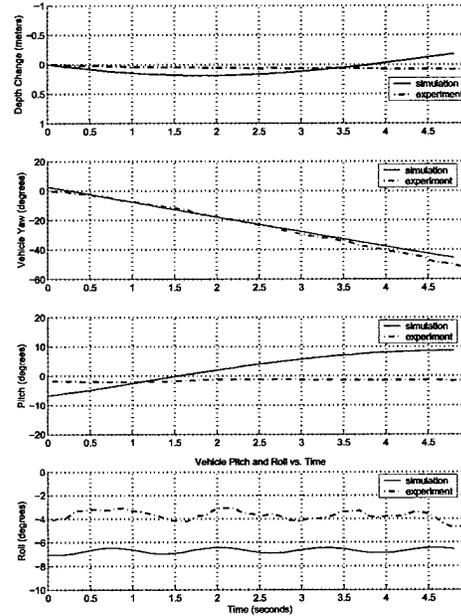Fig. 6: REMUS Simulator Data: Vehicle trajectory for vehicle response in the horizontal plane

Fig. 7: REMUS Simulator Data: Comparison plots for vehicle response in the yaw plane
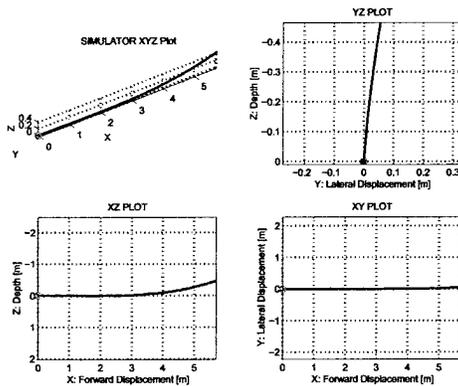
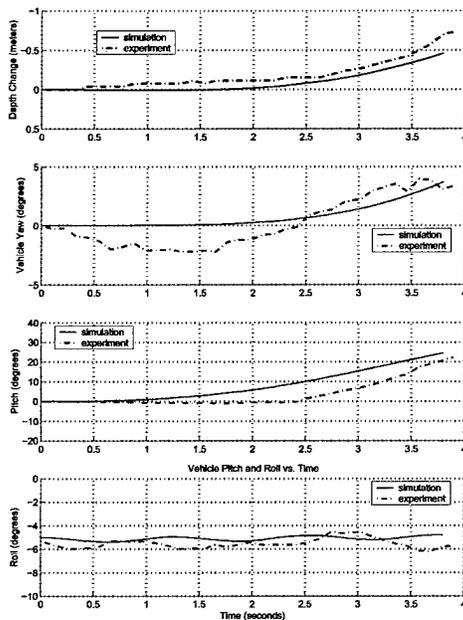Fig. 8: REMUS Simulator Data: Vehicle trajectory for vehicle pitching up

Fig. 9: REMUS Simulator Data: Comparison plots for vehicle pitching up

X. Conclusion

The vehicle dynamics model has been shown to accurately simulate the motion of the REMUS AUV, to the limit of the existing vehicle sensors. For a detailed description of the model development and experimental results, please refer to the author's MIT Master's thesis [13].

References

[1] B. Allen, W. Vorus, and T. Prestero. Propulsion system performance enhancements on REMUS AUVs. In *Proceedings MTS/IEEE Oceans 2000*, Providence, Rhode Island, September 2000. 2

[2] Robert D. Blevins. *Formulas for Natural Frequency and Mode Shape*. Kreiger Publishing, Florida, 1979. 2

[3] M. R. Bottaccini. The stability coefficients of standard torpedoes. NAVORD Report 3346, U.S. Naval Ordnance Test Station, China Lake, CA, 1954. 2

[4] J. Feldman. Revised standard submarine equations of motion. Report DTNSRDC/SPD-0393-09, David W. Taylor Naval Ship Research and Development Center, Bethesda, MD, June 1979. 2

[5] John E. Fidler and Charles A. Smith. Methods for predicting submersible hydrodynamic characteristics. Report NCSC TM-238-78, Naval Coastal Systems Laboratory, Panama City, FL, 1978. 2

[6] Thor I. Fossen. *Guidance and Control of Ocean Vehicles*. John Wiley & Sons, New York, 1994. 2

[7] M. Gertler and G. Hagen. Standard equations of motion for submarine simulation. Report DTNSRDC 2510, David W. Taylor Naval Ship Research and Development Center, Bethesda, MD, June 1967. 1

[8] Sighard F. Hoerner. *Fluid Dynamic Drag*. Published by author, 1965. 2

[9] Sighard F. Hoerner and Henry V. Borst. *Fluid Dynamic Lift*. Published by author, second edition, 1985. 2

[10] D. E. Humphreys. Development of the equations of motion and transfer functions for underwater vehicles. Report NCSL 287-76, Naval Coastal Systems Laboratory, Panama City, FL, July 1976. 2

[11] D. F. Myring. A theoretical study of body drag in subcritical axisymmetric flow. *Aeronautical Quarterly*, 27(3):186–94, August 1976. 1

[12] J. N. Newman. *Marine Hydrodynamics*. MIT Press, Massachusetts, 1977. 2

[13] Timothy J. Prestero. Verification of a six-degree of freedom simulation model for the REMUS AUV. Master's thesis, Massachusetts Institute of Technology/Woods Hole Oceanographic Institution, Departments of Ocean and Mechanical Engineering, 2001. 6

[14] M. Purcell, C. von Alt, B. Allen, T. Austin, N. Forrester, R. Goldsborough, and R. Stokey. New capabilities of the REMUS autonomous underwater vehicle. In *Proceedings MTS/IEEE Oceans 2000*, Providence, Rhode Island, September 2000. 1

[15] C. von Alt, B. Allen, T. Austin, and R. Stokey. Remote environmental monitoring units. In *Proceedings MTS/IEEE Oceans 1994*, Cambridge, MA, 1994. 1

[16] C. von Alt and J.F. Grassle. LEO-15: An unmanned long term environmental observatory. In *Proceedings MTS/IEEE Oceans 1992*, Newport, RI, 1992. 1

[17] L. F. Whicker and L. F. Fehlner. Free-stream characteristics of a family of low-aspect ratio control surfaces. Technical Report 933, David Taylor Model Basin, 1958. NC. 2

[18] D. R. Yoerger, J.G. Cooke, and J.-J. E. Slotine. The influence of thruster dynamics on underwater vehicle behavior and their incorporation into control system design. *IEEE Journal of Oceanic Engineering*, 15:167–178, July 1990. 2